

# KOI-372: a young extrasolar system with two giant planets on wide and eccentric orbits

L. Mancini<sup>1,2</sup>, J. Lillo-Box<sup>3</sup>, J. Southworth<sup>4</sup>, L. Borsato<sup>5</sup>,  
D. Gandolfi<sup>6,7</sup>, S. Ciceri<sup>1</sup>, D. Barrado<sup>3</sup>, R. Brahm<sup>8,9</sup>, and Th. Henning<sup>1</sup>

<sup>1</sup> Max Planck Institute for Astronomy, Königstuhl 17, 69117 – Heidelberg, Germany  
e-mail: [mancini@mpia.de](mailto:mancini@mpia.de)

<sup>2</sup> INAF – Osservatorio Astrofisico di Torino, via Osservatorio 20, 10025 – Pino Torinese, Italy

<sup>3</sup> Depto. de Astrofísica, Centro de Astrobiología (CSIC-INTA), ESAC campus 28691 – Villanueva de la Cañada, Spain

<sup>4</sup> Astrophysics Group, Keele University, Keele ST5 5BG, UK

<sup>5</sup> Dip. di Fisica e Astronomia “Galileo Galilei”, Università di Padova, Vicolo dell’Osservatorio 2, 35122 – Padova, Italy

<sup>6</sup> Dip. di Fisica, Università di Torino, via P. Giuria 1, 10125 – Torino, Italy

<sup>7</sup> Landessternwarte Königstuhl, Zentrum für Astronomie der Universität Heidelberg, Königstuhl 12, 69117 – Heidelberg, Germany

<sup>8</sup> Instituto de Astrofísica, Pontificia Universidad Católica de Chile, Av. Vicuña Mackenna 4860, 7820436 – Macul, Santiago, Chile

<sup>9</sup> Millennium Institute of Astrophysics, Av. Vicuña Mackenna 4860, 7820436 – Macul, Santiago, Chile

Preprint online version: October 15, 2018

## ABSTRACT

We confirm the planetary nature of KOI-372 b (aka Kepler object of interest K00372.01), a giant transiting exoplanet orbiting a solar-analog G2 V star. The mass of KOI-372 b and the eccentricity of its orbit were accurately derived thanks to a series of precise radial velocity measurements obtained with the CAFE spectrograph mounted on the CAHA 2.2-m telescope. A simultaneous fit of the radial-velocity data and *Kepler* photometry revealed that KOI-372 b is a dense Jupiter-like planet with a mass of  $M_p = 3.25 \pm 0.20 M_{\text{Jup}}$  and a radius of  $R_p = 0.882 \pm 0.088 R_{\text{Jup}}$ . KOI-372 b is moving on a quite eccentric orbit,  $e = 0.172 \pm 0.079$ , making a complete revolution around its parent star in 125.6 days. The semi-major axis of the orbit is  $0.4937 \pm 0.0085$  au, implying that the planet is close to its habitable zone ( $\sim 0.5$  au from it). By analysing the mid-transit times of the 12 transit events of KOI-372 b recorded by the *Kepler* spacecraft, we found a clear transit time variation, which is attributable to the presence of a planet c in a wider orbit. We estimated that KOI-372 c has a mass between 0.13 and 0.31  $M_{\text{Jup}}$ , also revolving on an eccentric orbit ( $e = 0.17 - 0.24$ ) in roughly 460 days, at a mean distance of  $\sim 1.2$  au from the host star, within the boundaries of its habitable zone. The analysis of the CAFE spectra revealed a relatively high photospheric lithium content,  $A(\text{Li}) = 2.48 \pm 0.12$  dex, suggesting that the parent star is relatively young. From a gyrochronological analysis, we estimate that the age of this planetary system is  $1.0 \pm 0.3$  Gyr.

**Key words.** stars: planetary systems – stars: fundamental parameters – stars: individual: KOI-372

## 1. Introduction

The transiting extrasolar planet (TEP) population turns out to be the best *atout* in the hands of exoplanetary scientists. Thanks to the early ground-based systematic surveys (e.g., Bakos et al. 2004; Alonso et al. 2004; McCullough et al. 2005; Pollacco et al. 2006; Pepper et al. 2007; Bakos et al. 2013) and then to those from the space (CoRoT: Barge et al. 2008, *Kepler*: Borucki et al. 2011), more than 1200 transiting planetary systems have now been found. The possibility to easily derive most of their physical and orbital parameters, and to investigate even the composition of their atmosphere, make the TEPs the most suitable targets to detect and study in detail. They currently represent the best statistical sample to constrain the theoretical models of planetary formation and evolution. Moreover, transit time variation (TTV) studies allowed the detection of additional non-transiting bodies in many TEP systems, highlighting the great efficacy of high-precision

and high-cadence photometry in the search for extrasolar planets.

The majority of TEPs have been discovered by the *Kepler* space telescope, which has revealed how varied they are, in terms of mass and size, and how diverse their architectures can be, confirming science-fiction pictures in several cases or going beyond human imagination in others.

Here we focus our attention on the *Kepler* system KOI-372. Thanks to precise RV measurements, we confirm the planetary nature of KOI-372 b (aka K00372.01, KIC 6471021), a massive gas-giant planet moving on an eccentric and wide orbit around a young and active G2 V star ( $V = 12.6$  mag). Moreover, we discover the existence of an additional less-massive giant planet, KOI-372 c, in the system.

## 2. Observations and data analysis

### 2.1. Kepler photometry

The *Kepler* spacecraft monitored KOI-372 from quarters 0 to 17 (i.e. four years; from May 2009 to May 2013). It was labelled as a *Kepler* object of interest (KOI) due to a  $\sim 0.2\%$  dimming in its light curve with a period of  $\sim 125$  days (Borucki et al. 2011). This periodic dimming is actually caused by the transit of a Jupiter-like planet candidate, KOI-372b, moving on a quite wide orbit around the star. 12 transits of KOI-372b are present in the *Kepler* long cadence (LC) light curves. We have labelled them from cycle -5 to cycle 6 (see Fig. 1). Two of the transits are incomplete (cycles -2 and -1); two are most likely contaminated by star spots (cycles -5 and 2); three were also covered in short cadence (SC) (cycles 4, 5 and 6). The complete *Kepler* light curve is shown in Fig. 2, which highlights a significant stellar variability ( $0.0470 \pm 0.0002$  mmag peak-to-peak). McQuillan et al. (2013) found a periodic photometric modulation in the light curve and, by assuming that it is induced by a star-spot activity, estimated a stellar rotation period of  $11.769 \pm 0.016$  days. This value is in good agreement with that found by Walkowicz & Basri (2013a,b), i.e.  $11.90 \pm 3.45$  days.

### 2.2. Radial velocity follow-up observations

We monitored KOI-372 between July 2012 and July 2014 with the Calar Alto Fibre-fed Echelle spectrograph (CAFE; Aceituno et al. 2013) mounted on the 2.2m telescope at the Calar Alto Observatory (Almería, Spain) as part of our follow-up programme of *Kepler* candidates. This programme has already confirmed the planetary nature of Kepler-91b (Lillo-Box et al. 2014a,b), Kepler-432b (Ciceri et al. 2015), Kepler-447b (Lillo-Box et al. 2015b), and has identified and characterised some false positives and fast rotators in the sample of *Kepler* planet candidates (Lillo-Box et al. 2015a). CAFE has a spectral coverage from 4000 Å to 9500 Å, divided into 84 orders with a mean spectral resolution of  $R = 63\,000$ . We acquired 21 spectra, which were reduced using the dedicated pipeline provided by the observatory (Aceituno et al. 2013). We used thorium-argon (ThAr) exposures obtained after each science spectrum to wavelength-calibrate the corresponding data. The final spectra have signal-to-noise ratios in the range  $S/N = 7\text{--}16$ . A radial velocity (RV) was obtained from each spectrum by using the cross-correlation technique through a weighted binary mask (Baranne et al. 1996). The mask is composed of more than 2000 sharp and isolated spectral lines in the CAFE wavelength range. The cross-correlation was performed in a  $\pm 30\text{ km s}^{-1}$  range around the expected RV of the star. The peak of the cross-correlation function (CCF) was measured by fitting a four-term Gaussian profile. This velocity was then corrected for the barycentric Earth radial velocity at mid-exposure time. Since we took several consecutive spectra, we decided to combine the RV values of the corresponding pairs in the cases where their individual signal-to-noise was low (i.e.,  $S/N < 10$ ) and mutual discrepancies were larger than  $50\text{ m s}^{-1}$ . This procedure can also diminish the effect of the stellar activity on the radial velocity (although here the expected amplitudes are of the order of few tens of  $\text{m s}^{-1}$ ). The final RV values and their observing times are shown in Table 1 and are compatible

with the presence of a  $\sim 3 M_{\text{Jup}}$  planet in the system (see Fig. 6 and Sect. 4).

**Table 1.** RV and BVS measurements of KOI-372 from CAHA/CAFE.

Date of observation BJD(TDB)-2450000	RV ( $\text{km s}^{-1}$ )	err <sub>RV</sub> ( $\text{km s}^{-1}$ )	BVS ( $\text{km s}^{-1}$ )
6116.529138	9.821	0.028	-0.098
6116.563805	9.802	0.029	-0.091
6124.382383	9.858	0.032	-0.064
6124.418231	9.842	0.019	-0.150
6127.383919	9.845	0.019	-0.124
6523.446917	9.890	0.038	-0.307
6598.287980	9.972	0.047	-0.158
6804.542906	10.073	0.027	-0.118
6821.633450	10.092	0.040	-0.117
6834.419426	10.037	0.025	-0.020
6840.528320	9.995	0.026	-0.300
6859.565660	9.853	0.026	-0.300

### 2.3. Spectral analysis and the age of KOI-372

We derived the spectroscopic parameters of the host star KOI-372 from the co-added CAFE spectrum, which has a S/N ratio of about 40 per pixel at 5500 Å. Following the procedures described in Gandolfi et al. (2013, 2014), we used a customised IDL<sup>1</sup> software suit to fit the composite CAFE spectrum to a grid of synthetic theoretical spectra. The latter were calculated with the stellar spectral synthesis program SPECTRUM (Gray & Corbally 1994) using ATLAS9 plane-parallel model atmospheres (Kurucz 1979), under the assumptions of local thermodynamic equilibrium (LTE) and solar atomic abundances as given in Grevesse & Sauval (1998). We fitted spectral features that are sensitive to different photospheric parameters. Briefly, we used the wings of the Balmer lines to estimate the effective temperature  $T_{\text{eff}}$  of the star, and the Mg I 5167, 5173, and 5184 Å, the Ca I 6162 and 6439 Å, and the Na I D lines to determine the surface gravity  $\log g_{\star}$ . The iron abundance  $[\text{Fe}/\text{H}]$  and microturbulent velocity  $v_{\text{micro}}$  was derived by applying the method described in Blackwell & Shallis (1979) on isolated Fe I and Fe II lines. To determine the macroturbulent velocity  $v_{\text{macro}}$ , we adopted the calibration equations for solar like stars from Doyle et al. (2014). The projected rotational velocity  $v \sin i_{\star}$  was measured by fitting the profile of several clean and unblended metal lines<sup>2</sup>. We found that KOI-372 has an effective temperature of  $T_{\text{eff}} = 5820 \pm 80\text{ K}$ ,  $\log g_{\star} = 4.4 \pm 0.1$  (cgs),  $[\text{Fe}/\text{H}] = -0.01 \pm 0.07$  dex,  $v_{\text{micro}} = 1.1 \pm 0.1\text{ km s}^{-1}$ ,  $v_{\text{macro}} = 3.2 \pm 0.6\text{ km s}^{-1}$ , and  $v \sin i_{\star} = 4.4 \pm 0.5\text{ km s}^{-1}$  (Table 3). According to the Straizys & Kuriliene (1981) calibration scale for dwarf stars, the effective temperature of KOI-372 translates to a G2V spectral type.

The CAFE co-added spectrum of KOI-372 reveals the presence of a moderate Li I 6707.8 Å absorption doublet (Fig. 3). We estimated the photospheric lithium abun-

<sup>1</sup> The acronym IDL stands for Interactive Data Language and is a trademark of ITT Visual Information Solutions.

<sup>2</sup> Here  $i_{\star}$  refers to the inclination of the stellar rotation axis with respect to the line of sight.

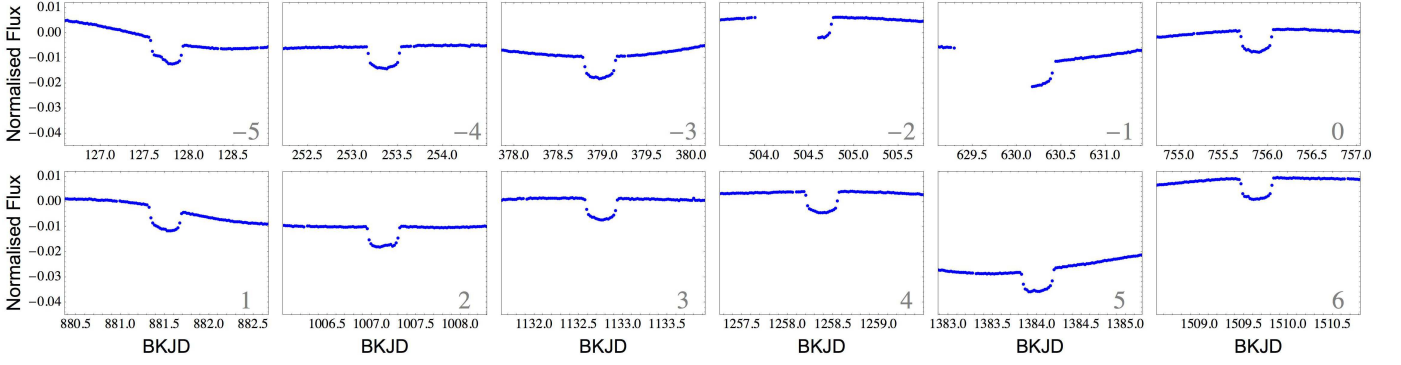


**Fig. 1.** The 12 transit events of KOI-372 b observed by *Kepler*. The transits at epoch -5 and 2 are affected by star-spot-crossing events. Times are in BKJD (Barycentric Kepler Julian Date – equivalent to BJD(TDB) minus 2454833.0).

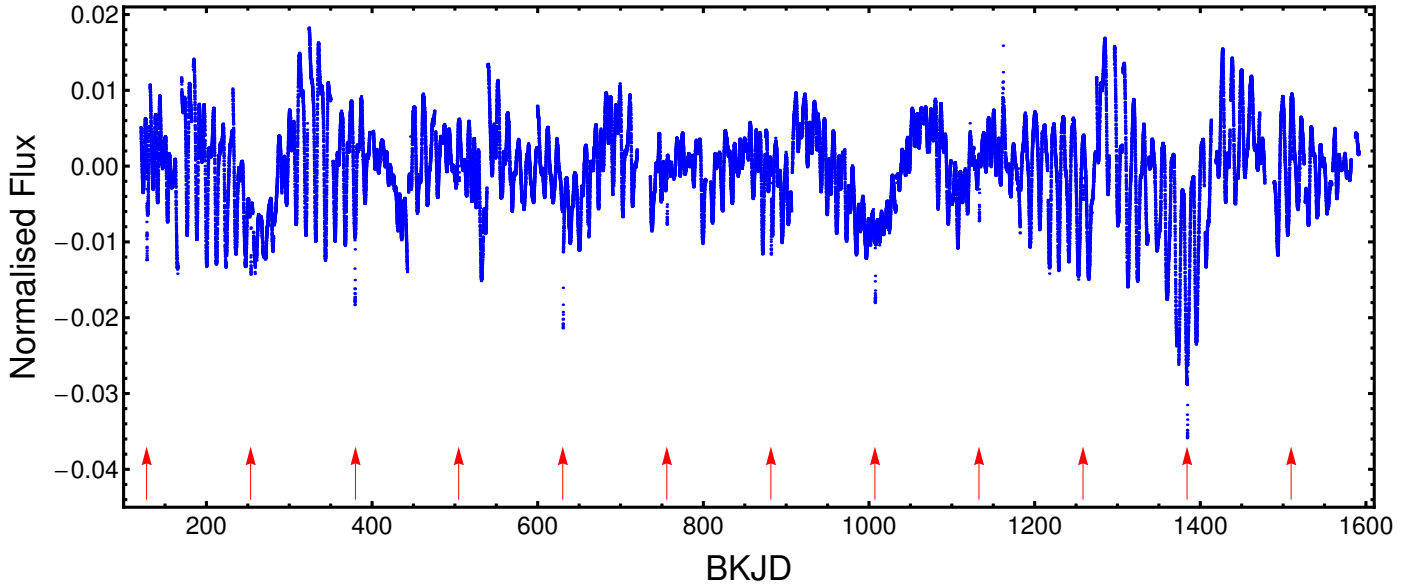


**Fig. 2.** The entire *Kepler* light-curve data of KOI-372. The large stellar variability can be reasonable interpreted as induced by a star-spot activity. Times are in BKJD (Barycentric Kepler Julian Date – equivalent to BJD(TDB) minus 2454833.0). The red arrows mark the mid-times of the twelve transits of KOI-372 b.

dance of the star by fitting the Li doublet using ATLAS9 LTE model atmospheres. We fixed the stellar parameters to the values given in Table 3 and allowed our code to fit the lithium content. Adopting a correction for non-LTE effects of  $+0.006$  dex (Lind et al. 2009), we measured a lithium abundance of  $A(\text{Li}) = \log(n(\text{Li})/n(\text{H})) + 12 = 2.48 \pm 0.12$  dex.

The photospheric lithium content and the short rotation period of KOI-372 suggest that the star is relatively young. Fig. 4 shows the lithium abundance of KOI-372 compared to the  $A(\text{Li})$  of the dwarf stars of the Pleiades, Hyades, and NGC 752 open clusters, as listed in Soderblom et al. (1993), Pace et al. (2012), and Sestito et al. (2004), respectively. KOI-372 has to be older than  $\sim 0.1$  Gyr, as the star falls below the envelope of the Pleiades. Although lithium depletion becomes ineffective beyond an age of 1–2 Gyr (Sestito & Randich 2005), KOI-372 lies between the envelopes of the other two clusters, suggesting an age intermediate between the age of the Hyades ( $\sim 0.6$  Gyr) and

the age of NGC 752 ( $\sim 2.0$  Gyr). This is further confirmed by the fact that the lithium content of KOI-372 is intermediate between the average lithium abundance measured in early G-type stars of 0.6-Gyr-old open clusters ( $A(\text{Li}) = 2.58 \pm 0.15$  dex) and that of 2-Gyr-old open clusters ( $A(\text{Li}) = 2.33 \pm 0.17$  dex; Sestito & Randich 2005).

We used Eq. (32) from Barnes (2010) and the rotation period of KOI-372 to infer its gyro-age, assuming a convective turnover time-scale of  $\tau_c = 34$  days (Barnes & Kim 2010) and a zero-age main-sequence rotation period of  $P_0 = 1.1$  days (Barnes 2010). We found a gyro-age of  $1.0 \pm 0.3$  Gyr, which confirms the relatively young scenario. Our estimation is in good agreement with the 1.15 Gyr gyro-chronological age predicted by Walkowicz & Basri (2013a,b).

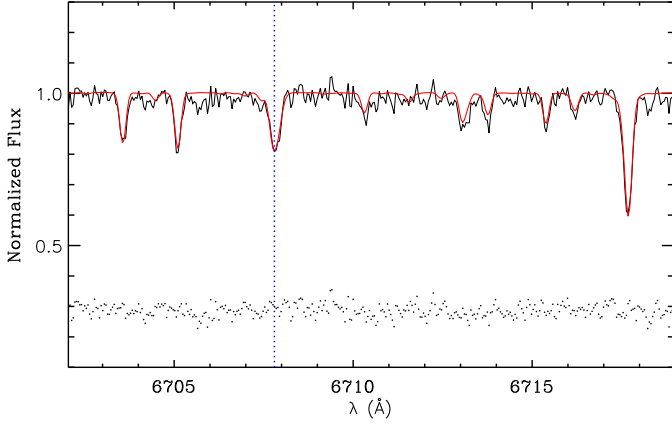


**Fig. 3.** CAFE co-added spectrum of KOI-372 (black line) encompassing the Li I 6707.8 Å absorption doublet. The best fitting ATLAS9 spectrum is overplotted with a thick red line. The vertical dashed line marks the position of the Li doublet. The lowest part of the plot displays the residuals to the fit.

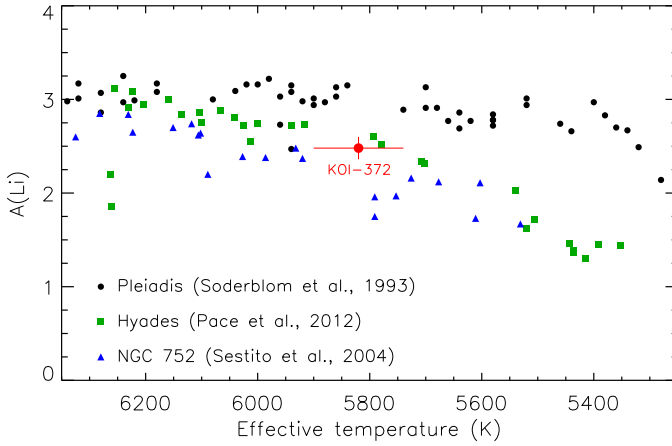


**Fig. 4.** Lithium abundances of F- and G-type dwarf stars in the Pleiades (black dots; Soderblom et al. 1993), Hyades (green squares; Pace et al. 2012), and NGC 752 (blue triangles; Sestito et al. 2004) open clusters. The red dot marks the position of KOI-372.

#### 2.4. Excluding false-positive scenarios

A faint pulsating variable star or a binary system in the background/foreground can mimic a planetary transit signal on the target star. High-resolution images are extremely useful to exclude this possibility (e.g., Lillo-Box et al. 2014c). A  $K_s$ -band, high-resolution, adaptive optics image of KOI-372 was obtained with ARIES on the 6.5 m MMT telescope by Adams et al. (2012), who found four stars within 6'' of the target, see Table 2. Following Lillo-Box et al. (2012), we have estimated the dilution effect caused by each companion, finding that it is very small for the three closest targets, roughly 0.023% in total and thus negligible. Concerning the very bright companion “E”, this is another object targeted as KIC 6471028. As it lies outside the *Kepler* aperture, this star does not contaminate KOI-372. KIC 6471028 was also detected with the AstraLux North instrument mounted on the CAHA

**Table 2.** Nearby visual companions around KOI-372 (from Adams et al. 2012) and their dilution effect on the depth of the transit events.

Companion	Distance (")	$K_s$ (mag)	$\Delta K_s$	Dilution
B	2.49	23.2	8.6	0.005 %
C	3.56	22.4	8.0	0.01 %
D	4.99	22.7	8.2	0.008 %
E <sup>a</sup>	5.94	17.1	4.0	1.31 %

**Notes.** <sup>a</sup>Also known as KIC 6471028.

2.2 m telescope by Lillo-Box et al. (2012), who estimated that this is a K2-K4 background dwarf.

An intense stellar activity could mimic the presence of a planetary body in the RV signal, thus causing a false positive case. We have also analysed such a possibility by determining the bisector velocity span (BVS) from the CAFE spectra (the values are reported in Table 1). The bisector analysis provides a Pearson correlation coefficient between the RV and the BVS of 0.081, which corresponds to a two-sided tail probability of 80%, that is less than 1- $\sigma$  significance for a positive correlation.

### 3. Physical properties of the system

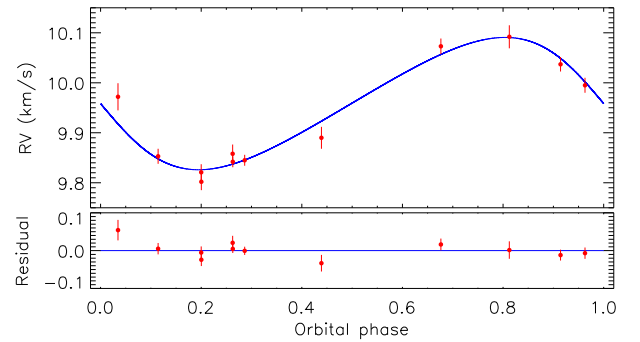


**Fig. 6.** Upper panel: phased RVs for KOI-372 and the best fit from JKTEBOP. Lower panel: residuals of RVs versus best fit.

For the determination of the physical parameters of the KOI-372 system, we proceeded as in Ciceri et al. (2015). We first selected for analysis all data within two transit durations of a transit, ignoring the two with only partial coverage in the *Kepler* light curve, and converted from flux to magnitude units. Each transit was then detrended by fitting a polynomial versus time. High polynomial orders of 3 to 5 were required to account for the brightness variations of the host star caused by spot activity.

We then fitted the photometry and the CAFE RV measurements simultaneously using the JKTEBOP code (Southworth 2013), after modifying it to allow fitting for individual times of mid-transit. The *Kepler* LC and SC data were fitted separately, accounting for the long effective exposure times in the LC data by oversampling the fitted model by a factor of five. The following parameters were fitted: the fractional radii of the two objects ( $r_* = R_*/a$  and  $r_p = R_p/a$ , where  $a$  is the orbital semi-major axis), the orbital inclination  $i$ , the time of midpoint of each tran-

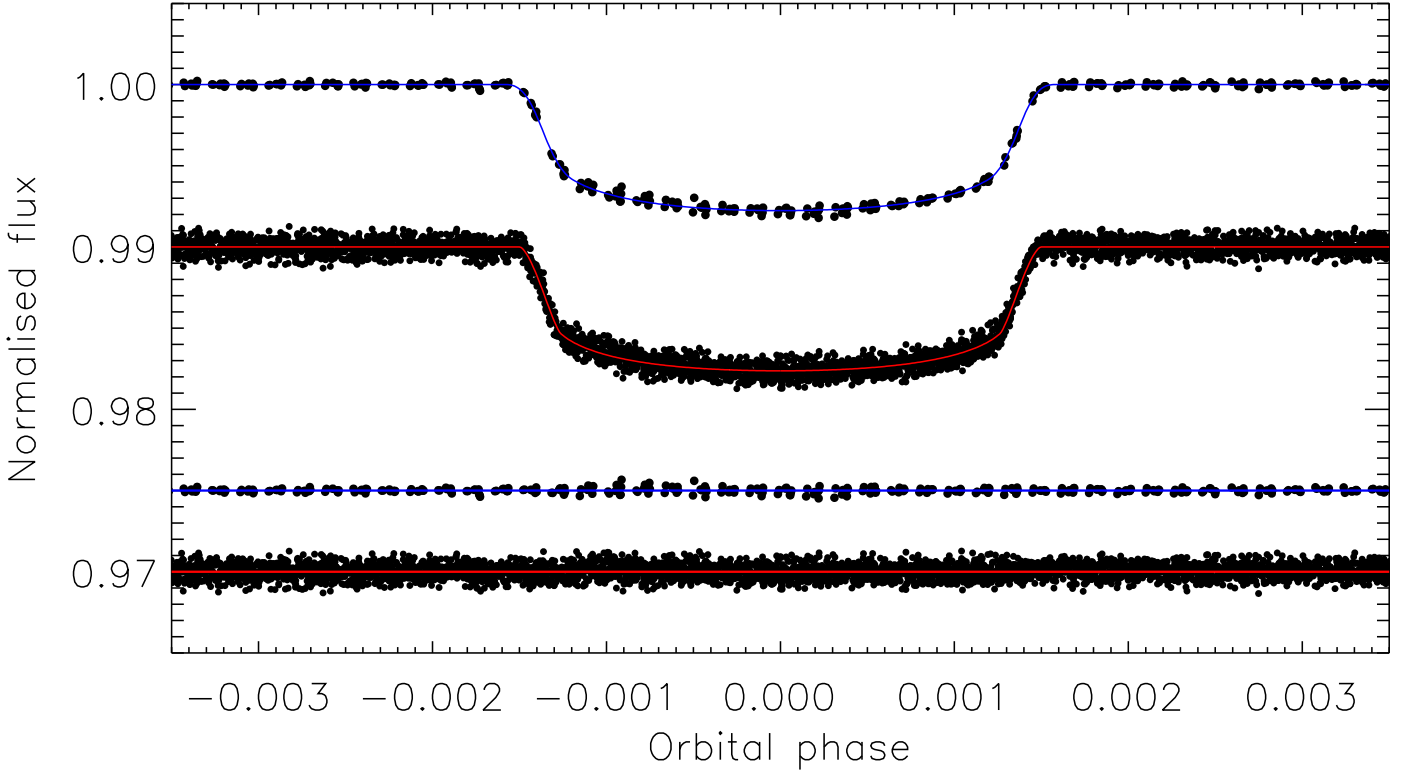


**Fig. 5.** Phased Kepler long-cadence (top light curve) and short-cadence (bottom light curve) data zoomed around transit phase. The TTVs (see Sect. 4) were removed from the data before plotting. The JKTEBOP best fits are shown using solid lines. The residuals of the fits are plotted at the base of the figure.

sit, the velocity amplitude  $K_*$ , the systemic velocity  $V_\gamma$ , the orbital eccentricity  $e$  and the argument of periastron  $\omega$ , via the combination terms  $e \cos \omega$  and  $e \sin \omega$ , and the coefficients of the polynomial for each transit. The orbital period  $P_{\text{orb}}$  and reference transit midpoint  $T_0$  were fixed to the values measured from the transit times; these were used only for phasing the RV measurements. A quadratic limb darkening law was used, with the linear term fitted and the quadratic term fixed to 0.27 (Sing 2010). We rescaled the error bars of the LC, SC and RV data to give a reduced  $\chi^2$  of  $\chi_\nu^2 = 1.0$  for each versus the fitted model.

The best fits to the photometry and the RVs are shown in Figs. 5 and 6. The uncertainties in the fitted parameters were derived by running both Monte Carlo and residual-permutation simulations (Southworth 2008) and choosing the larger of the two error bars for each parameter. The results obtained using the SC data are more precise than those from the LC data, so were adopted as the final set of photometric parameters.

We estimated the physical properties of the system from the SC results and the  $T_{\text{eff}}$  and  $[\text{Fe}/\text{H}]$  measured from our spectra. Constraints from theoretical stellar models were used to make the solution determinate. We followed the HSTEP approach (Southworth 2012, and references therein), which yielded measurements of the properties of the star and planet accompanied by both statistical and systematic errorbars. The results are reported in Table 3 and show that KOI-372b is a dense Jupiter-like planet on a wide and eccentric orbit.

The reader might wonder why the stellar and planetary radii are so uncertain ( $\sim 10\%$ ), given the quality of the Kepler transit light curve. This is due to the uncertainty

of the spectroscopic orbit, which compromises the  $r_A + r_b$  value measured from the light curve. Even though we know the transit duration with a good accuracy, the orbital speed of the planet at the time of transit is a bit uncertain, implying that the radius of the star is also uncertain. Since  $R_p$  is linked to  $R_*$  through  $k$ , the planet radius becomes uncertain as well.

#### 4. Planet KOI-372 c from transit time variation

We have analysed the 12 mid-transit times of KOI-372b to characterise the ephemeris of the transit and check if there is a possible transit time variation (TTV), which could be a sign of the presence of additional bodies in this system. Since the transits at cycles -5 and 2 are quite affected by star spots, we fitted them with the PRISM<sup>3</sup> and GEMC<sup>4</sup> codes (Tregloan-Reed et al. 2013, 2015). The mid-transit times for the other epochs were estimated using JKTEBOP. The resulting timings are tabulated in Table 4 and were fitted with a straight line to obtain the orbital period,  $P_{\text{orb}} = 125.63243 \pm 0.00071$  days, and the reference time of mid-transit,  $T_0 = 2455588.8710 \pm 0.0030$  BJD (TDB). A plot of the residuals around the fit (see Fig. 7) shows a clear deviation from the predicted transit times, meaning that the orbital period of KOI-372b is variable. The uncertainties of  $P_{\text{orb}}$  and  $T_0$  have been increased to account for this, but we stress that these values should be used with caution. We analysed the possibility that the observed TTV is induced by undetected spot crossing events.

<sup>3</sup> Planetary Retrospective Integrated Star-spot Model.

<sup>4</sup> Genetic Evolution Markov Chain.

**Table 3.** Final parameters of the planetary system KOI-0372.

Parameter	Nomen. and Unit	Value
<i>Stellar parameters</i>		
R.A. (J2000) .....		19 <sup>h</sup> 56 <sup>m</sup> 29.39 <sup>s</sup>
Dec. (J2000) .....		41°52′00.3″
Kepler magnitude .....	$K_p$ (mag)	12.39
Effective temperature ..	$T_{\text{eff}}$ (K)	5820 ± 80
Iron abundance .....	[Fe/H] (dex)	−0.01 ± 0.07
Lithium abundance ....	A(Li) (dex)	2.5 ± 0.1
Microturb. velocity ....	$v_{\text{micro}}$ (km s <sup>−1</sup> )	1.1 ± 0.1
Macroturb. velocity <sup>a</sup> ..	$v_{\text{macro}}$ (km s <sup>−1</sup> )	3.2 ± 0.6
Proj. rotat. velocity ..	$v \sin i_*$ (km s <sup>−1</sup> )	4.4 ± 0.5
Age <sup>b</sup> .....	(Gyr)	1.0 ± 0.3
Spectral type <sup>c</sup> .....		G2 V
Rotation period <sup>d</sup> .....	$P_{\text{rot}}$ (day)	11.769 ± 0.016
Mass .....	$M_*$ ( $M_{\odot}$ )	1.014 ± 0.044 ± 0.027
Radius .....	$R_*$ ( $R_{\odot}$ )	1.122 ± 0.083 ± 0.010
Mean density .....	$\rho_*$ ( $\rho_{\odot}$ )	0.72 ± 0.16
Surface gravity .....	$\log g_*$ (cgs)	4.344 ± 0.065 ± 0.004
<i>Planetary parameters (KOI-372 b)</i>		
Mass .....	$M_p$ ( $M_{\text{Jup}}$ )	3.25 ± 0.19 ± 0.06
Radius .....	$R_p$ ( $R_{\text{Jup}}$ )	0.882 ± 0.088 ± 0.008
Mean density .....	$\rho_p$ ( $\rho_{\text{Jup}}$ )	4.4 ± 1.4 ± 0.1
Surface gravity .....	$g_p$ (m s <sup>−2</sup> )	103 ± 21
Equilibr. temperature ..	$T_{\text{eq}}$ (K)	423 ± 16
<i>Orbital parameters</i>		
Time of mid-transit ....	$T_0$ (BJD <sub>TDB</sub> )	2455588.8710 ± 0.0030
Period .....	$P_{\text{orb}}$ (days)	125.63243 ± 0.00071
Semi-major axis .....	$a$ (au)	0.4937 ± 0.0073 ± 0.0044
Inclination .....	$i$ (degree)	89.845 ± 0.086
Fractional star radius ..	$r_A$	0.01057 ± 0.00078
Fractional planet radius	$r_b$	0.000854 ± 0.000085
RV semi-amplitude ....	$K_A$ (m s <sup>−1</sup> )	132.3 ± 6.3
Barycentric RV .....	$\gamma$ (km s <sup>−1</sup> )	9.959 ± 0.007
Eccentricity .....	$e$	0.172 ± 0.079
Argum. of Periastron ..	$\omega$ (degree)	791 ± 16

**Notes.** Where there are two error bars, the first is a statistical error, coming from the measured spectroscopic and photometric parameters, while the second is a systematic error and is given only for those parameters which have a dependence on theoretical stellar models.

<sup>a</sup> Using the calibration equations of Doyle et al. (2014).

<sup>b</sup> From gyrochronology.

<sup>c</sup> With an accuracy of ± 1 sub-class.

<sup>d</sup> From McQuillan et al. (2013).

Following the method described in Mazeh et al. (2015), we found that there is no significant correlation between the observed TTV and the local slope of the light curve at the transit times, suggesting that the TTV is likely induced by an unseen companion.

In order to identify the origin of this TTV we used the TRADES (TRANSITS and Dynamics of Exoplanetary Systems; Borsato et al. 2014) code, which allows modelling of the dynamics of multiple planet systems by reproducing the observed mid-transit times and RVs, with the possibility to choose among four different algorithms. We ran two series of simulations, the first by selecting the PIKAIA algorithm (Charbonneau 1995), the second with the Particle Swarm Optimization (PSO) algorithm (Tada 2007). In both the cases, we fixed tight boundaries for the parameters of planet **b** (centred on the values in Table 3) and investigated four different configurations:

**Table 4.** *Kepler* times of transit midpoint of KOI-372b and their residuals.

Time of minimum BJD(TDB)−2400000	Cycle no.	Residual (JD)
54960.74947 ± 0.00109	−5	0.040612
55086.35000 ± 0.00040	−4	0.008712
55212.96694 ± 0.00042	−3	−0.006781
55337.57977 ± 0.00043	−2	−0.026380
55463.23346 ± 0.00118	−1	−0.005126
55588.87808 ± 0.00041	0	0.007068
55714.51794 ± 0.00043	1	0.014495
55840.13340 ± 0.00096	2	−0.002478
55965.77212 ± 0.00043	3	0.003803
56091.39778 ± 0.00030	4	−0.002963
56217.00030 ± 0.00030	5	−0.001233
56342.66701 ± 0.00030	6	0.001403

**Table 5.** Parameters of KOI-372c from the TRADES best fits of the *Kepler* mid-transit times and CAFE RV measurements.

Parameter	Unit	PIKAIA	PSO
<b>KOI-372 c</b>			
$M_p$	$M_{\text{Jup}}$	0.1348 <sup>+0.0020</sup> <sub>−0.0021</sub>	0.3194 <sup>+0.0034</sup> <sub>−0.0026</sub>
$P_{\text{orb}}$	days	457.57 <sup>+0.42</sup> <sub>−0.41</sub>	463.44 <sup>+0.25</sup> <sub>−0.25</sub>
$e$		0.2440 <sup>+0.0015</sup> <sub>−0.0017</sub>	0.1701 <sup>+0.0016</sup> <sub>−0.0017</sub>
$\omega$	degree	308.77 <sup>+0.27</sup> <sub>−0.25</sub>	178.88 <sup>+0.86</sup> <sub>−0.90</sub>
$i$	degree	97.92 <sup>+0.59</sup> <sub>−0.68</sub>	91.78 <sup>+1.17</sup> <sub>−1.28</sub>

**Notes.** Two series of simulations run by using the PIKAIA algorithm (Charbonneau 1995) and the Particle Swarm Optimization (PSO) algorithm (Tada 2007), respectively.

- i) planet **b** + planet **c** with  $0.1 < P_{\text{orb}} < 250$  days;
- ii) planet **b** + planet **c** with  $225 < P_{\text{orb}} < 500$  days;
- iii) planet **b** + planet **c** with  $0.1 < P_{\text{orb}} < 1000$  days;
- iv) planet **b** + planet **c** with  $130 < P_{\text{orb}} < 500$  days + planet **d** with  $0.1 < P_{\text{orb}} < 1000$  days.

The solutions obtained from the TRADES fitting processes were further analysed using the Frequency Map Analysis (FMA; Laskar et al. 1992) to check if they are stable. Both the algorithms found that the stable solution that best fits the data is that for the configuration (ii). The configuration (iv) with three planets also gave a good fit to the data, but the FMA analysis indicated that it is unstable. The PIKAIA and PSO solutions indicate that KOI-372c has a mass of between 0.13 and 0.32  $M_{\text{Jup}}$ , and has a wide orbit with  $P_{\text{orb}} = 456\text{--}463$  days, and eccentricity  $e = 0.17\text{--}0.24$ . The final parameters, with confidence intervals estimated with a bootstrapping method, are reported in Table 5.

## 5. Discussion and conclusions

Thanks to precise RV measurements obtained with the high-resolution spectrograph CAFE, we confirmed the planetary nature of KOI-372b, a dense Jupiter-like planet with a mass of  $3.25 \pm 0.20 M_{\text{Jup}}$  and a radius of  $0.882 \pm 0.088 R_{\text{Jup}}$ , revolving with a period of 125.6 days on a quite eccentric orbit ( $e = 0.172 \pm 0.079$ ) around a G2 V star, similar to the Sun. The parameters of the parent star and



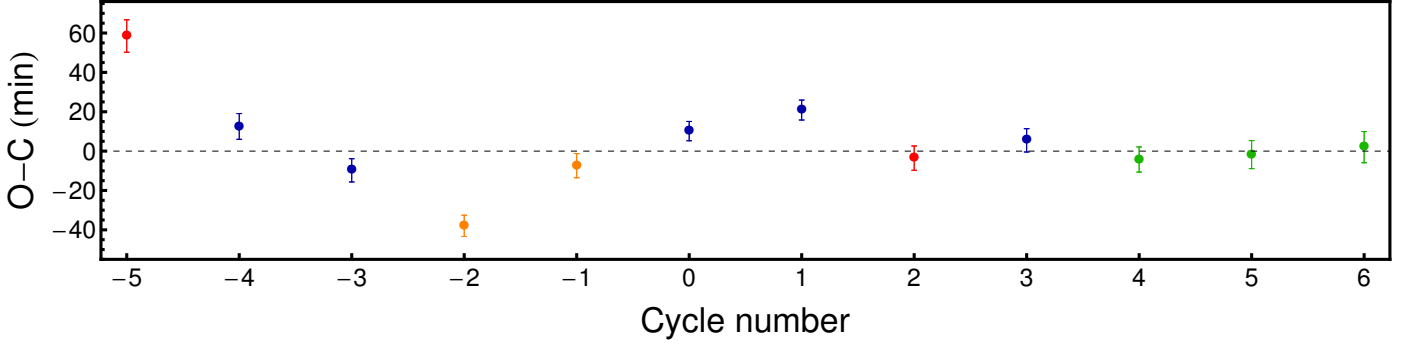


**Fig. 7.** O–C diagram for the timings of KOI-372 b at mid-transit versus a linear ephemeris. The timings in blue refer to those coming from the *Kepler* LC data, while those marked with green are from SC data. The red points refer to the two LC transits affected by star spots. The two incomplete LC transits are marked with orange points.

the planet were obtained by analysis of the CAFE spectra, and a joint fit to the RV data and *Kepler* transit light curves. Orbiting at  $\sim 0.5$  au from its host, KOI-372 b is located close to its *habitable zone* (HZ), which has a width of  $\sim 0.72$  au, as we estimated it based on the stellar parameters reported in Table 3 and the HZ calculator by Kopparapu et al. (2013, 2014). The parent star is quite active, as is shown by the 0.047 mmag peak-to-peak modulation present in the long time-series photometry and from the star-spot anomalies clearly visible in two of the transit events monitored by *Kepler*. Even though it has physical characteristics that resemble those of the Sun, KOI-372 is much younger:  $1.0 \pm 0.3$  Gyr as estimated from its lithium abundance and gyrochronology.

The host star is relatively bright and therefore amenable for exoplanet atmosphere studies. Even though the orbit is quite eccentric, the star-planet distance should always be large enough to consider KOI-372 b as a non-inflated planet with a low irradiation level. Since there are only a handful of transiting Jupiter-like planets with a low irradiation level, this planetary system could be a precious target to future studies of exoplanet atmosphere of normal giant gas planets.

An analysis of the *Kepler* mid-transit times of KOI-372 b revealed a clear TTV signal. We studied this with TRADES, a code able to make a simultaneous fit of RV and mid-transit times and compare the results with simulated data of various multi-planetary configurations. We found that the TTV can be explained through the presence of a  $0.13\text{--}0.32 M_{\text{Jup}}$  super-Neptune-like planet c on a wider orbit than that of KOI-372 b, with an orbital period between 457 and 463 days. The orbit of KOI-372 c is eccentric ( $e = 0.17\text{--}0.24$ ) and quite coplanar ( $i = 91^\circ\text{--}97^\circ$ ). Such a system is stable according to the results of an FMA analysis. Using Kepler’s third law, we estimated that the semi-major axis of the orbit of KOI-372 c is  $\sim 1.2$  au.

We have also analysed the possibility that planet c can transit the host star. First, we assumed that the orbit of planet c is completely coplanar with that of planet b, i.e.  $i_c = i_b = 89.85 \pm 0.09$ , and simulated 1000 orbits in the corresponding uncertainties of the parameters, obtaining that the probability of transit is 83%. Then, we assumed that planet c stays on a more inclined orbit, as that coming from the PSO solution of the TTV analysis, see Table 5. In this case, the simulations provided a transit probability of 7%, which is low but not negligible. A Neptune-size planet should produce a  $\sim 800$  ppm transit on this star. However, a

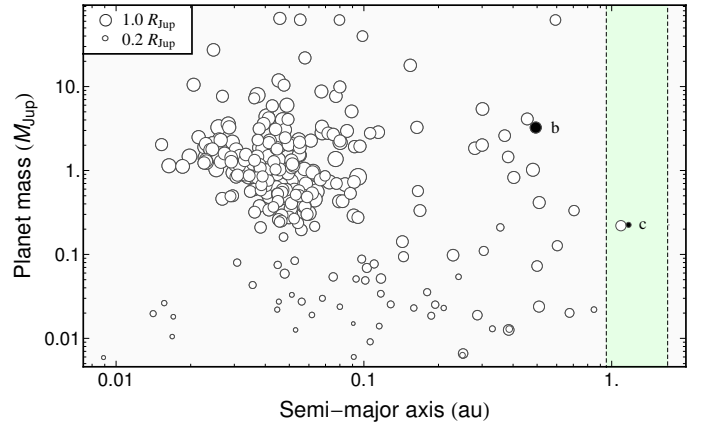


**Fig. 8.** The *semi-major axis–planetary mass* diagram for transiting planets. The size of each circle is proportional to the corresponding planetary radius (data taken from TEPcat). The black circles indicate the position of KOI-372 b and KOI-372 c (the size of the circle that marks the position of KOI-372 c is arbitrary as we do not know its radius). The error bars have been suppressed for clarity. The green region delimited by the two vertical dashed lines delimits the HZ of KOI-372.

careful analysis of the entire *Kepler* light curve did not give evidence of any clear transit of depth more than 200 ppm, with the exception of those related to KOI-372 b. This implies that KOI-372 c does not transit in front of the parent star and that the orbits of the two planets are not exactly coplanar.

Given its young age, the physical parameters of this planetary system can be very precious for astrophysicists working on theories of planet formation and evolution. If we visualise the known transiting planets, reported in TEPcat<sup>5</sup>, in a semi-major axis–mass diagram (Fig. 8), we can see that KOI-372 b and KOI-372 c occupy sparsely-populated regions of this plot (here for the mass of KOI-372 c we have considered the mean value between those estimated by the two different simulations, see Table 5). In particular, KOI-372 c is in the HZ of its host star. This fact could be interesting in the hypothesis that this planet has some moons (Kipping et al. 2012) or small rocky co-orbital terrestrial bodies (Ford & Gaudi 2006), which might then

<sup>5</sup> TEPcat (Transiting Extrasolar Planet Catalogue) is available at [www.astro.keele.ac.uk/jkt/tepcat/](http://www.astro.keele.ac.uk/jkt/tepcat/) (Southworth 2011).

be habitable. Unfortunately, the parameters of KOI-372c are not well constrained as they are based on a poorly-sampled TTV (only 12 transit timings). More transit observations of KOI-372b are required to accurately measure the properties of its smaller brother.

**Acknowledgements.** This paper is based on observations collected with the 2.2 m Telescope at the Centro Astronómico Hispano Alemán (CAHA) in Calar Alto (Spain) and the publicly available data obtained with the NASA space satellite *Kepler*. Operations at the Calar Alto telescopes are jointly performed by the Max-Planck-Institut für Astronomie (MPIA) and the Instituto de Astrofísica de Andalucía (CSIC). This research has been partially funded by Spanish grant AYA2012-38897-C02-01. J.L.-B. thanks the CSIC JAE-predoc program for Ph.D. fellowship. R.B. is supported by CONICYT-PCHA/Doctorado Nacional. R.B. acknowledges additional support from project IC120009 “Millennium Institute of Astrophysics (MAS)” of the Millennium Science Initiative, Chilean Ministry of Economy. We acknowledge the use of the following internet-based resources: the ESO Digitized Sky Survey; the TEPCat catalogue; the SIMBAD data base operated at CDS, Strasbourg, France; and the arXiv scientific paper preprint service operated by Cornell University.

## References

- Aceituno, J., Sánchez, S. F., Grupp, F., et al. 2013, *A&A*, 552, A31
- Adams, E. R., Ciardi, D. R., Dupree, A. K., et al. 2012, *AJ*, 144, 42
- Alonso, R., Brown, T. M., Torres, G., et al. 2004, *ApJ*, 613, 153
- Bakos, G. Á., Noyes, R. W., Kovács, G., et al. 2004, *PASP*, 116, 266
- Bakos, G. Á., Csabry, Z., Penev, K., et al. 2013, *PASP*, 125, 154
- Baranne, A., Queloz, D., Mayor, M., et al. 1996, *A&AS*, 119, 373
- Barge, P., Baglin, A., Auvergne, M., et al. 2008, *A&A*, 482, L17
- Barnes, S. A. 2010, *ApJ*, 722, 222
- Barnes, S. A. & Kim, Y.-C. 2010, *ApJ*, 721, 675
- Blackwell, D. E., Shallis M. J. 1979, *MNRAS*, 186, 673
- Borsato, L., Marzari, F., Nascimbeni, V., et al. 2014, *A&A*, 571, A38
- Borucki, W. J., Koch, D., Basri, G., et al. 2011, *ApJ*, 736, 19
- Charbonneau, P. 1995, *ApJS*, 101, 309
- Ciceri, S., Lillo-Box, J., Southworth, J., et al., 2015, *A&A*, 573, L5
- Doyle, A. P., Davies, G. R., Smalley, B., et al. 2014, *MNRAS*, 444, 3592
- Ford, E. B., & Gaudi, B. S. 2006, *ApJ*, 652, L137
- Gandolfi, D., Parviainen, H., Fridlund, M. et al., 2013, *A&A*, 557, AA74
- Gandolfi, D., Parviainen, H., Deeg, H. J. et al., 2014, *arXiv:1409.8245*
- Gray R. O., Corbally C. J., 1994, *AJ*, 107, 742
- Grevesse, N., Sauval, A. J., 1998, *SSRv*, 85, 161
- Kipping, D. M., Bakos, G. Á., Buchhave, L. A., et al. 2012, *ApJ*, 750, 115
- Kopparapu, R. K., Ramirez, R., Kasting, J. F., et al. 2013, *ApJ*, 765, 131
- Kopparapu, R. K., Ramirez, R., SchottelKotte, J., et al. 2014, *ApJ*, 787, L29
- Kurucz R. L. 1979, *ApJS*, 40, 1
- Laskar, J., Froeschlé, C., Celletti, A. 1992, *Physica D*, 56, 253
- Lillo-Box, J., Barrado, D., Bouy, H. 2012, *A&A*, 546, A10
- Lillo-Box, J., Barrado, D., Moya, A., et al. 2014a, *A&A*, 562, A109
- Lillo-Box, J., Barrado, D., Henning, Th., et al. 2014b, *A&A*, 568, L1
- Lillo-Box, J., Barrado, D., Bouy, H. 2014c, *A&A*, 566, A103
- Lillo-Box, J., Barrado, D., Mancini, L., et al. 2015a, *A&A*, 576, A88
- Lillo-Box, J., Barrado, D., Santos, N. C., et al. 2015b, *A&Ain press*, *arXiv:1502.03267*
- Lind, K., Asplund, M., Barklem, P. S., 2009, *A&A*, 503, 541
- Mazeh, T., Holczer, T., Shporer, A. 2015, *ApJ*, 800, 142
- McCullough, P. R., Stys, J. E., Valenti, J. A., et al. 2005, *PASP*, 117, 783
- McQuillan, A., Mazeh, T., Aigrain, S. 2013, *ApJ*, 775, L11
- Pace, G., Castro, M., Meléndez, J., et al. 2012, *A&A*, 541, A150
- Pepper, J., Pogge, R. W., DePoy, D. L., et al. 2007, *PASP*, 119, 923
- Pollacco, D. L., Skillen, I., Collier Cameron, A., et al. 2006, *PASP*, 118, 1407
- Sestito, P., Randich, S., Pallavicini, R. 2004, *A&A*, 426, 809
- Sestito, P., Randich, S. 2005, *A&A*, 442, 615
- Sing, D. 2010, *A&A*, 510, A21
- Soderblom, D. R., Jones, B. F., Balachandran, S., et al. 1993, *AJ*, 106, 1059
- Southworth, J. 2008, *MNRAS*, 386, 1644
- Southworth, J. 2011, *MNRAS*, 417, 2166
- Southworth, J. 2011, *MNRAS*, 426, 1291
- Southworth, J. 2013, *A&A*, 557, A119
- Straizys, V. & Kuriliene, G. 1981, *Ap&SS*, 80, 353
- Tada, T. 2007, *Journal of Japan Society of Hydrology & Water Resources*, 20, 450
- Takeda, Y., Honda S., Ohnishi, T., et al. 2013, *PASJ*, 65, 53
- Tregloan-Reed, J., Southworth, J., Tappert, C. 2013, *MNRAS*, 428, 3671
- Tregloan-Reed, J., Southworth, J., Burgdorf, M. 2015, *MNRAS in press*, *arXiv:1503.09184*
- Walkowicz, L. M., & Basri, G. S. 2013a, *MNRAS*, 436, 1883
- Walkowicz, L. M., & Basri, G. S. 2013b, *VizieR On-line Data Catalog: J/MNRAS/436/1883*